Microglia-to-astrocyte communication modulates synaptic and cerebrovascular functions following traumatic brain injury

Juliana M Rosa[✉1,4]*, Victor Farre-Alins[1,2]*, Marta Navarrete[3], Alejandra Palomino-Antolin[1,2], Elena Fernandez-Lopez[4], Paloma Narros-Fernandez[1,2], Javier Egea[✉1,2]

[1] Research Unit, Hospital Santa Cristina. Instituto de Investigación Sanitaria Princesa (IIS-IP), Hospital Universitario de la Princesa, Madrid, Spain

[2] Instituto Teófilo Hernando and Departamento de Farmacología y Terapéutica, Facultad de Medicina, Universidad Autónoma de Madrid, Madrid, Spain

[3] Instituto Cajal, Consejo Superior de Investigaciones Científicas, Madrid 28002, Spain

[4] Hospital Nacional de Parapléjicos, Servicio de Salud de Castilla-La Mancha, 45071, Toledo, Spain

*Equally contribution

✉Corresponding Authors:

JM Rosa (current address): Hospital Nacional de Parapléjicos, Finca La Peraleda s/n, Research Unit, Planta 1, Lab 5, 45071, Toledo, Spain. Fax: +34 925 247745

e-mail: jmartinsd@externas.sescam.jccm.es

J Egea: Research Unit, Hospital Santa Cristina. C/ Maestro Vives, 2-3. 28009. Madrid, Spain

e-mail: javier.egea@inv.uam.es

Abstract

Activation of microglia and astrocytes contributes to synaptic remodeling, tissue repair and neuronal survival following traumatic brain injury (TBI). However, the consequences of the interaction between both glial cell types in rewiring neuronal networks and repairing brain functions remains poorly understood. Here, we explored how microglia-induced astrocyte activation modified synapses and cerebrovascular integrity following TBI. Calcium imaging experiments from brain slices revealed increased number of active astrocytes responding with spontaneous Ca^{2+} events surrounding the injury at 1 d.a.i. These changes correlated with an increase in astrocytic GFAP-reactivity and microglia activation. Blocking microglia activation with the TLR4-blocker TAK242 reduced both the number of active and reactive astrocytes, suggesting a role for microglia in mediating astrocyte excitability. To determine the physiological consequences of microglia-induced astrocyte activation, we first quantified the number of synaptic puncta in TBI-mice treated with the TLR4-blocker. PSD-95/VGlut-1 staining showed that TAK-treatment reduced by half the synaptic loss observed in TBI-mice. Similar effects were also observed in the blood-brain barrier (BBB) integrity, in which blockage of microglia decreased Evans Blue extravasation, an indicative of preserved BBB. The acute effects of microglia inhibition on synapses and BBB were not observed in $IP_3R2^{-/-}$ mice, indicating that the microglial effects depend on the subsequent astrocyte activation. In addition, acute TBI increases the release of the astrocytic-protein thrombospondin-1 (TSP-1) that seems to be necessary to modulate synaptic puncta in a sub-acute phase. Together, our data demonstrate that microglia-to-astrocyte communication plays a crucial role in the pathophysiology of TBI and that its inhibition prevents the synaptic loss and BBB damage accelerating the recovery/repair of damaged tissue. Overall, our data indicates that targeting the microglia-astrocyte crosstalk might represent a therapeutic potential in CNS injuries and disorders.

Introduction

Traumatic brain injury (TBI) leads to a loss of neuronal function due to both cell death in the damaged tissue and cell dysfunction in the surrounding and remote brain areas (1,2). Recovery of function after TBI involves activation of cell repair mechanisms and initiation of the so-called neuronal plasticity. In the last few years, it has been shown that plasticity is not a mechanism involving solely neurons, but it depends on a more complex network including distinct cell types such as astrocytes and microglia. Astrocytes are the most abundant glial cells in the brain that respond to a vast array of CNS insults and diseases (i.e. acute trauma, infection and stroke) (3-5). The response of astrocytes to injury seems to be a major determinant of the outcome due to their role in the modulation of synaptic transmission and plasticity and regulation of neurovascular functions (2,6,7). Emerging evidence indicates that astrocytes exert either a neuroprotective or a neurotoxic function depending on the type of the insult or brain disease. In this way, neuroprotective effects of reactive astrocytes were observed in the control of the size of the injury core following brain injury (8); while detrimental effects of reactive astrocytes on synaptic number and debris phagocytosis were reported after ischemia or infection (8,9). The transformation of astrocytes to a neuroprotective or neurotoxic phenotype seems to depend on the activation of distinct microglial signaling (8,9), however it is still inconclusive the mechanisms controlling such dual role and the possible pathophysiological consequences.

Microglia is the constant sensor of changes in the CNS microenvironment and contributes to normal development, function and repair of the brain. Under pathological conditions or after an injury, microglia is rapidly activated and initiates an inflammatory response to restore tissue homeostasis. In addition, microglia activation determines the fate of astrocytes by releasing a plethora of signaling factors that induce reactive astrogliosis and regulate astrocytic immune reactions (10,11). On the other hand, activated astrocytes-derived factors also trigger microglial activation and control their cellular functions (12). In this way, microglia and astrocytes establish a bidirectional communication that is determinant for the fate of both cell types as well as for the function of neuronal networks. Previous reports have shown that the specific manipulation of astrocytes activity as well as microglia contributes to synaptic remodeling, tissue repair and neuronal survival (13-16); however little is still known about the consequences of the interaction between microglia-astrocyte in the rewiring of neuronal networks and in the repairing of brain

functions under pathological conditions. Here, we investigated the functional alterations of astrocytes induced by microglia activation and how microglia-astrocyte interaction regulates synapses and neurovascular unit after an acute traumatic brain injury. Our data show that in response to an acute TBI, there is a recruitment of excitable and reactive astrocytes surrounding the injured area induced by activation of microglial TLR4 signaling. Microglia-induced astrocyte activation exerts detrimental effects on synapses, blood-brain barrier and neurological outcome at 24 h post-injury. On the other hand, we also found that microglia activation shortly after TBI increases the release of the astrocytic protein thrombospondin-1 (TSP-1) that serves to control the homeostatic recovery of synapses few days after injury. Altogether, our data give evidence that microglia-astrocyte crosstalk plays an instructive role in neuronal networks by modulating the number of synapses and controlling blood-brain barrier damage, which may have important pathophysiological relevance for the long-term plasticity.

Methods

Animals: Experiments were carried out in accordance with the International Council for Laboratory Animal Science and the European Union 2010/63/EU Guidelines. The experimental protocol was approved by the Ethical Committee for Animal Research at the Hospital Nacional de Parapléjicos (Toledo, Spain) and by the Institutional Ethics Committee of Universidad Autónoma de Madrid, Spain. All experiments were performed on male and female C57BL/6J wild type and IP_3R2 knockout adult mice (2-3 months, 25-35 g weight). Animals were group-housed in a controlled temperature environment under a 12 h light/dark cycle, with access to food and water ad libitum. All efforts were made to minimize the number of animals used and their suffering.

Traumatic Brain Injury Model: The Closed Head Injury (CHI) adapted from (17) was used as a model of TBI in mice. Briefly, animals were anesthetized with isoflurane (induction at 5% and maintenance at 1%) and placed on a hard platform in order to minimize dissipation of energy. CHI was produced by a 50 g weight dropped from a height of 34 cm along a metal rod connected to a tip of 5 mm of diameter that hits the mice on the right hemisphere between sagittal and lambdoid sutures. After trauma, mice were immediately subjected to posttraumatic resuscitation (if necessary) and oxygen (2-3 liter O_2/min) administration until regular breath was restored.

Immunofluorescence and confocal imaging: For IHC, mice were perfused with PBS, and brains were excised and incubated in 4% paraformaldehyde for 24 hours before freezing in an embedding compound on dry ice. Frozen brains were cut with a cryostat (CM 1100; Leica) at 18 µm thickness. Sections were incubated overnight at 4°C with the primary Abs rabbit anti-GFAP (1:1,000; catalog AB5804; EMD Millipore); rabbit anti-Iba1 (1:1,000; catalog 019-19741; Wako); rabbit anti–PSD-95 (1:500; catalog 51-6900; Invitrogen); and guinea pig anti-VGlut1 (1:2,500; catalog AB230175; EMD Millipore), and then washed with PBS and further incubated for 3 hours at room temperature with the secondary Abs Alexa Fluor 488–, Alexa Fluor 546–, and Alexa Fluor 594–conjugated mouse/guinea pig and rabbit IgGs (all from Invitrogen). Immunofluorescence images were obtained using a confocal microscope with FLUOVIEW (Olympus). The number of colocalized synaptic puncta (VGlut1/PSD-95) was quantified as previously described (18). Briefly, 5-µm-thick confocal Z-stacks (optical section depth of 0.33

μm; 15 sections/Z-stack; imaged area measuring 11,272 μm^2) of the synaptic zone in S1 cortex were imaged. Maximum projections of 3 consecutive optical sections were generated from the original Z-stack. The number of pre-, post-, and colocalized synaptic puncta was quantified by using the Puncta Analyzer plugin (developed by Barry Wark and provided by Cagla Eroglu) for ImageJ software. Three image stacks per mouse (n = 4 mice/group) were used for analyses.

Calcium imaging acquisition and analysis: Animals were injected intraperitoneally with sulforhodamine 101 (SR101; 100 mg/kg) and left in the cage with food and water for 1–2 h before removing the brain (19). Ca^{2+} levels in astrocytes specifically loaded with SR101, were monitored by fluorescence microscopy using the Ca^{2+}indicator Fluo-4-AM (Molecular Probes, Eugene, OR; 2–5 μl of 2mM dye were dropped over S1 cortex, attaining a final concentration of 2–10 μM and 0.01% of pluronic acid, for 15–20 min at room temperature) (20). In these conditions, most of the cells loaded were astrocytes, as confirmed by their electrophysiological properties in (19). Thus, astrocytes monitored and analyzed in this study were those double labeling for SR101 and Fluo-4. Cells were imaged using a CCD camera attached to the microscope. Cells were illuminated with a CoolLED pE-100 fluorescent excitation system and images were acquired every 1-1.5 s using Scight software (Scientifica). Astrocytic Ca^{2+} signals were analyzed offline using SARFIA, a custom-written suite of macros running in Igor Pro (Wavemetrics) (21). Prior to analysis, images were registered to correct movements in the X and Y directions. Movies were rejected if the plane of focus altered significantly during imaging acquisition. Regions of Interest (ROIs) containing both soma and proximal ramifications were chosen using a filtering algorithm based on a Laplace operator and segmented by applying a threshold, as described in detail in (21,22). This algorithm defined most or all of the ROIs that an experienced observer would recognize by eye. Individual ROI responses were then normalized as the relative change in fluorescence ($\Delta F/F$), smoothed by binomial Gaussian filtering, and analyzed to detect activity using custom-made scripts based on a first derivate detection algorithm. A threshold set at ~1.5-2 times the standard deviation of the time derivative trace was used to detect changes in fluorescence within the ROIs. The reliability of this algorithm to detect calcium activity was first tested by comparing the results with manual activity detection. In this paper, the fluorescent intensity of ROIs is reported as the average intensity across all pixels within its area. Fluorescent responses are reported as normalized increases as follows:

$\Delta F/F=(F-F_o)/F_o$

where F is the instantaneous fluorescence induced by a spontaneous activity and F_o is the baseline fluorescence. The Ca^{2+} oscillation frequency was obtained from the number of Ca^{2+} transients occurring in 6 to 15 astrocytes in the field of view during 1 min of recording (23).

Neurological lesions assessment: The severity of the injury is based on the assessment of motor and neurobehavioral functions at 1 h and 24 h after trauma using the Neurological Severity Score (NSS) test, modified from (17). The score consists of the evaluation of 10 parameters, described below in Table 1. Animals with a score of 9-10 points were sacrificed considering it an endpoint criterion. NSS was assessed 1 hour and 24 hours after TBI and mice were sacrificed following the 24-hour test.

Table 1. Parameters evaluated in Neurological Severity Score (NSS) test. Success in each task is considered 0 points; failure is considered 1 point.

Task	*Description*
Exit circle	Exit a circle of 30 cm of diameter in 2 minutes
Seeking behavior	Interest in the environment and movement
Motor skills	Straight walk Monoparesis or hemiparesis
Startle reflex	Response to a loud hand clap
Beam balancing	Ability to balance on a surface of 10 x 10 mm
Beam walk	Cross a 30-cm long beam of 3 cm width Cross a 30-cm long beam of 2 cm width Cross a 30-cm long beam of 1 cm width
Round stick balancing	Ability to balance on a 5-mm round stick

Pharmacological treatment: Mice were randomly divided into 3 groups: (I) not-injured mice (sham group); (II) subjected to TBI and treated with 0.9% NaCl saline solution (saline group); (III) subjected to TBI and treated with the TLR4 inhibitor TAK242 diluted in saline containing

3% DMSO (3 mg/kg; Sigma-Aldrich) (TAK group). Animals were treated intraperitoneally (i.p.) immediately following the 1-hour NSS test.

Blood-Brain Barrier integrity: To evaluate the permeability of the blood-brain vessels and brain edema, 2% Evans Blue tracer (Sigma-Aldrich) diluted in saline was injected i.p. following the 1-hour NSS test. Animals were sacrificed 24 h after trauma and brains were extracted and sectioned in 2-mm slices using a mouse brain slicer. The slices were scanned and total area of Evans Blue extravasation was measured in each slice using ImageJ.

ELISA: S100-β levels were measured in plasma using a specific ELISA kit (MyBioSource, catalog MBS2500369) following the manufacturer's instructions. Blood was collected in the sacrifice of mice at 24 h after trauma in EDTA-treated tubes that were centrifuged at 5000 rpm during 10 minutes to obtain plasma.

Immunoblotting: Mice brain cortex was lysed in ice-cold lysis buffer (1% Nonidet P-40, 10% glycerol, 137mM NaCl, 20mM Tris–HCl, pH 7.5, 1 g/mL leupeptin, 1 mM PMSF, 20 mM NaF, 1 mM sodium pyrophosphate, and 1 mM Na_3VO_4). Proteins (30 µg) from brain cell lysate were resolved by SDS–PAGE and transferred to Immobilon-P membranes (Millipore Corp.). Membranes were incubated with anti-TSP1 (1:500; catalog MS-1066-P1, NeoMarkers) or anti-βactin (1:50000; catalog A3854, Sigma-Aldrich). Appropriate peroxidase-conjugated secondary antibodies (1:10000; Santa Cruz Biotechnology) were used to detect proteins by enhanced chemiluminescence. Different band intensities corresponding to immunoblot detection of protein samples were quantified using the Scion Image program. Immunoblots correspond to a representative experiment.

Statistics: Group measurements are expressed as mean ± SD. We used *t* tests to compare two groups and one-way ANOVA to compare more than two groups. The level of significance was set at $p < 0.05$.

Results

FIGURE 1

Traumatic brain injury induces astrocyte reactivity and microglia activation in somatosensory cortex

Activation of microglia has been recently linked to the induction of reactive astrocytes with neurotoxic (9) or neuroprotective (8) effects after brain lesions and neurodegenerative diseases. We then investigated whether an acute TBI also leads to microglia-induced cortical astrocyte reactivity in a closed head injury (CHI) mice model that allows for a biomechanics similar to human TBI (17,24). For that, we first confirmed the presence of astrocytes and microglia activation in mice that received moderate unilateral CHI over the somatosensory (S1) and motor cortical areas (Fig. 1A). Cresyl violet-stained CHI injured tissues (Fig. 1A, a'') showed substantial cortical damage at 24 h post-injury with no overt subcortical damage compared with sham animals (Fig. 1A, a'). TBI and sham brains were then immunostained against GFAP or Iba-1 to mark astrocyte or microglia reactivity, respectively (Fig. 1B-D). A significant increase in $GFAP^+$ astrocytes was observed at 300-400 μm of the injured area of the ipsilateral S1 cortex at 1 d.a.i, with only few $GFAP^+$ cells in sham or in contralateral S1 cortex (Fig. 1C), corroborating previous reports showing absence of astrogliosis in cortical areas with no apparent damage (8). We next examined microglia activation after CHI. When microglia became active and enter in an inflammatory state, their morphologies switch from a resting status (ramified type with small cell bodies and thin projections) to an activated form (hypertrophic type with large cell bodies and shorter and thicker projections or bushy type showing enlarged cell bodies with multiple short process that form thick bundles) (25). Microglia from the surrounding injured tissue displayed thicker processes and enlarged cell bodies compared to sham or contralateral cortex (Fig. 1B, D), indicating that TBI led to an increase in the microglia activated state. When unbiased analysis was performed to classify microglial phenotypes, we found that TBI decreased the resting type (ramified), whiles increased the activated type (both hypertrophic and bushy) in the ipsilateral S1 cortex (Fig. 1D). These data indicate that microglia morphology changes from a resting to an active state that well match the time point in which astrocyte also become reactive following TBI as previously described (8). Therefore, CHI model used in this study induces the characteristic microglia activation and astrocyte reactivity previously showed in others TBI models.

FIGURE 2

Since microglia activation precedes astrocyte reactivity, we seek a way to inhibit microglia to manipulate the interaction between microglia and astrocyte in order to explore the pathophysiological consequences of microglia-induced astrocyte activation. Toll like receptors type 4 (TLR4) are expressed specifically by microglial cells in the rodent CNS as shown by genetic profiles of pure astrocyte and microglia population (9). TLR4 activation by damaged-associated molecules released after brain injuries or neuroinflammation mediates microglia activation (9,26-28). In addition, TLR4 activation was also observed to initiate microglia-induced astrocyte activation in response to external damage signals (4,9). We then tested whether the blockage of microglial-TLR4 receptors could be used as a tool to inhibit microglia and the subsequent astrocytes activation in our CHI model. For that, we pharmacologically blocked TLR4 receptors by treating TBI animals with the TAK242 (3 mg/kg, Fig. 2A) or vehicle 1 hour after injury. Immunostaining quantification of GFAP and Iba1 markers from TBI brains collected 1 d.a.i. showed a decrease in the number of both $GFAP^+$ astrocytes and activated microglial surrounding the injured area as compared to those control or vehicle-treated mice (Fig. 2B-D). Together, these data indicate the efficacy of the TLR4 blockage to decrease microglia-astrocyte interaction following an acute TBI.

FIGURE 3

Acute traumatic brain injury increases the population of cortical astrocytes with somatic Ca^{2+} transients

Reactive astrocytes are known to result in a spectrum of morphological and molecular changes that can influence injury progression and recovery (6,29,30); however, little is known about the changes in functional activity of reactive astrocytes that could affect further synaptic stability and neuronal networks. Using epifluorescence microscope imaging, we examined basal somatic Ca^{2+} transients from astrocytes localized nearby the damaged area (Fig. 3A) of the ipsilateral and contralateral S1 cortex of TBI and sham mice. We then measured the spontaneous Ca^{2+} transients from astrocytes loaded with the astrocytic marker sulforhodamine 101 (SR101) and the

intracellular calcium dye Fluo4-AM (Fig. 3B). Spontaneous Ca^{2+} transients were defined as a change in fluorescence intensity relative to baseline. We observed that the proportion of "active astrocytes" showing 1 or more Ca^{2+} transients during the 1-min recording period were markedly increased in the ipsilateral cortex of TBI mice at 1 d.a.i. as compared to those in the contralateral cortex or sham animals (Fig. 3C). These effects were independent of neuronal activity, as TTX did not prevent the increase in active astrocyte population (data not shown, ipsi *vs* ipsi TTX $p = 0.2$). We also found that the frequency of spontaneous astrocyte Ca^{2+} transients were unchanged in TBI mice as compared to sham animals or contralateral cortex (Fig. 3D, E). These results indicate that acute TBI leads to important functional changes in cortical astrocytes observed as an increase in the number of responsive cells nearby the injury rather than an intrinsic increase in the astrocytic Ca^{2+} transients or extension of intracellular Ca^{2+} network.

Blockage of microglia activation decreases reactivity and spontaneous Ca^{2+} transients in TBI cortical astrocytes.

We next tested whether the recruitment of astrocytes responding with Ca^{2+} oscillations in the peri-injured cortical area after TBI was dependent on microglia activation. TBI mice were treated with the TLR4 blocker TAK242 (3 mg/kg) to reduce microglial activation and astrocyte activity (Fig. 3F). Supporting our anatomical results, we observed that TAK-treated mice had dramatically decreased number of active astrocytes in the ipsilateral S1 cortex as compared to those vehicle-treated group (Fig. 3G). No changes in the frequency of Ca^{2+} oscillations within active astrocytes were observed (Fig. 3H). These results indicate that microglia activation plays a crucial role in triggering anatomical and functional changes in S1 astrocytes following an acute brain injury.

FIGURE 4

Control of microglia-induced astrocyte reactivity prevents blood-brain barrier damage after TBI

Once confirmed that the increase in astrocytes responding with Ca^{2+} transients surrounding the injured area is induced by microglia activation (Fig. 1-3), we asked what are the physiological consequences of such microglia-astrocyte crosstalk in the pathophysiology of TBI. As a first

approach, we investigated the alterations in the blood-brain barrier (BBB) integrity, which is highly regulated by astrocytes and dramatically disrupted following an acute TBI (2,12,31,32). First, we quantified the amount of the astrocytic marker S100β that is released into the plasma following disruption of the BBB and used in the clinic as a biomarker of BBB damage (i.e. higher the severity of BBB disruption, more S100β in serum is found). ELISA measurements showed increased amount of S100β in the serum collected 1 d.a.i. (Fig. 4A), indicating elevated astrocyte activity and/or damage. Pharmacological treatment with the microglial TLR4-blocker TAK242 significantly decreased the concentration of S100β, corroborating a role for microglia activation in the astrocyte modulation. We then injected Evans Blue dye intraperitoneally into the TBI-mice and assessed BBB integrity by measuring the amount of dye leakage into the brain parenchyma (Fig. 4B). Evans blue dye leakage in TBI-mouse brains was mostly detected around the lesion area of the ipsilateral cortex, with very low dye leakage levels in the contralateral cortex (Fig. 4B-C). We then treated mice with the microglial TLR4-blocker TAK242 to inhibit microglia-astrocyte communication and found less amount of dye-stained areas compared with those vehicle-treated mice (Fig. 4B-C), indicating that microglia activation after TBI exacerbates BBB damage. Evans blue dye leakage was not detected in sham-control mice (data not shown). We then used the inositol 1,4,5-trisphosphate receptor type 2 knockout mice (*Itpr2*$^{-/-}$, herein referred to as $IP_3R2^{-/-}$) to test whether the effect on BBB integrity was directly related to astrocyte or microglia. IP3R2 is selectively expressed in astrocytes, and astrocyte somatic Ca^{2+} transients are absent in these mice line (33,34). $IP_3R2^{-/-}$ animals also presented increased dye leakage in the ipsilateral cortex compared to contralateral cortex (Fig. 4C). On contrary to what observed in WT animals, TAK242 treatment of $IP_3R2^{-/-}$ did not lesser the amount of Evans Blue extravasation following TBI, indicating the crucial effect of the microglia-induced astrocyte activation in the BBB integrity. Taking together, our results suggest that astrocyte-microglia interaction has a detrimental role in the BBB preservation after TBI, and inhibition of microglia activity reduces BBB damage.

Changes in the number of synaptic puncta density in S1 cortex after TBI

Microglia and astrocytes are known to influence neuronal transmission through the regulation of synapses and the modulation of neuronal network (16,35-37). To further investigate the physiological consequences of microglia-astrocyte crosstalk in the pathophysiology of TBI, we

determined to which degree the interaction between these two cell types regulates synaptic formation. For that, we quantified the synaptic density surrounding the injured cortex by double immunostaining for pre- and postsynaptic proteins, i.e. the number of colocalized presynaptic VGlut1 and postsynaptic PSD-95 puncta, in sham and TBI groups 1 d.a.i. We defined the normalized synaptic density as the ratio of synapses in the surrounding TBI area to that in the homotopic non-injured contralateral cortex to correct for any endogenous differences. Our results showed that ipsilateral S1 cortex from TBI mice had significantly less synapses compared to sham mice (35 ± 5% decrease ipsi-TBI vs sham, $p = 0.0092$; 37 ± 4 decrease ipsi-TBI vs contra-TBI, $p = 0.0072$, Fig. 4D-E). We then treated TBI mice with the microglial TLR4 blocker (TAK242) and found reduced loss of PSD-95/VGlut1 punctas in TAK-treated mice compared to vehicle-treated mice (Fig. 4D-E). These data indicate that inhibition of microglia activation shortly after TBI either restores synaptic level or inhibits synaptic loss. We next quantified the number of synaptic puncta in TBI brain from $IP_3R2^{-/-}$ mice to test whether the neuroprotective effect on synapses observed after pharmacological blockage of microglia was exerted either by a direct effect of microglia or by the microglia-induced astrocyte activation. Synaptic density was quantified as before to avoid endogenous differences. $IP_3R2^{-/-}$ mice presented decreased synaptic loss following TBI compared to sham animals. In addition, pharmacological treatment of $IP_3R2^{-/-}$ mice with TAK242 did not recover the number of synapses (Fig. 4E). These data indicate a role of astrocytes on the control of synaptic number following TBI.

Figure 5

TSP-1 astrocyte release regulates synaptic number in the sub-acute phase of TBI

Since the mechanisms controlling microglia and astrocyte activation are known to have distinct phases from hours to days after injury (38), we determined the anatomical and functional changes of microglia-induced astrocyte activation 7 d.a.i (Fig. 5A). We first analyzed the changes in astrocytes activation and reactivity. Calcium imaging experiments from TBI cortex revealed similar number of active astrocytes and Ca^{2+} oscillation frequency as compared to those sham or contralateral cortex (Fig. 5B). A significant increase in the number of $GFAP^{+}$ astrocytes was still observed 7 d.a.i. (Fig. 5C), but such increase was smaller than those found 1 d.a.i ($p = 0.049$).

Second, we quantified the number of activated microglia to determine if the decrease in astrocyte excitability correlated with changes in microglia activation. Although an increase in the activated and a decrease in the resting type was observed 7 d.a.i. in the ipsilateral cortex, it was much less than the observed 1 d.a.i. (Fig. 5C). Finally, we determined the levels of synaptic co-localization 7 d.a.i and found similar number of synapses in TBI mice to those sham (Fig. 5D), indicating a synaptic recovery in a sub-acute phase. The later corroborates previous anatomical and electrophysiological findings showing an initial loss of synapses and a decrease in neuronal excitability followed by its gradual homeostatic recovery after ischemic stroke or TBI in mice (1,31,39-41). Altogether, our data indicate a homeostatic recovery of microglia and astrocyte activity that correlates to increased number of synapses.

Figure 6

We next sought to identify the potential molecular mechanism that causally links astrocyte activation to homeostatic synaptic regulation at 7 d.a.i. We focused on TSP-1, which is an astrocyte-secreted soluble protein that is necessary and sufficient to promote the formation of synapses during neuronal development or following brain damage (31,42). Western blot analysis showed increased expression of TSP-1 in the ipsilateral S1 cortex 1 d.a.i., which returned to basal levels 7 d.a.i. (Fig. 6A) (31,43). Blockage of the microglial TLR4-signalling significantly reduced TSP-1 expression to levels similar to sham or contralateral tissues, indicating that microglia activation following TBI controls TSP-1 release from astrocytes. To investigate whether the transient up-regulation of TSP-1 protein within the first few hours after TBI was linked to the synaptic remodeling observed 7 days post-injury, we used the $IP_3R2^{-/-}$ mice known to have reduced release of TSP-1 after injuries (13) and quantified synaptic puncta from TBI brains 7 d.a.i. Our co-localization analysis showed that the number of synaptic puncta in $IP_3R2^{-/-}$ TBI brain did not recover 7 d.a.i. (Fig. 6B), indicating the important role of astrocyte activation in the homeostatic regulation of synapses in a sub-acute phase through the release of TSP-1.

Figure 7

Blockage of microglia-induced astrocyte activation improves functional outcome in TBI mice

Synaptic damage is thought to be a major contributor to neurological symptoms and behavioral deficits following acute brain injuries. Given the significant effect on synapses and BBB integrity, we explored the possibility that activation of microglia-astrocyte interaction might also affect neurological behavior associated with TBI. We therefore investigated whether TAK242 treatment improved functional outcome by subjecting animals to a neurological severity score (NSS), a battery of behavioral tests specifically developed to assess motor and neurobehavioral outcome in TBI mice (17). The NSS is highly correlated with the severity of brain damage – being a score of 10 points a maximal neurological impairment and 0 is a no damage. As expected, TBI mice presented significantly higher neurological deficits as early as 1 h post-injury. When we examined the temporal evolution of functional deficit, we found that the performance of TBI mice gradually recovered, but still significantly worse at 1 d.a.i. (Fig. 6C). We then inhibited the microglia signaling to astrocytes by treating TBI mice with the TLR4-pathway blocker TAK242 or vehicle and performed the same NSS test. Administration of TAK242 partially reversed the neurological deficit, accelerating the recovery of neurological motor functions in TBI mice when compared to those animals treated only with the vehicle. In addition, TAK242 treatment did not lead to partial recovery of NSS score in $IP_3R2^{-/-}$ mice. These data demonstrate that blockage of the microglia-induced astrocyte activation has beneficial effects on early neurological motor tests following TBI.

Discussion

We here identified a fine-tune interaction of microglia-astrocyte which modulates the number of synapses and BBB damage with pathophysiologic relevance for long-term plasticity in traumatic brain injury. We show that acute TBI produces a recruitment of excitable astrocytes surrounding the damaged area in a TLR4-dependent manner (Fig. 1-3 and Fig. 7). Microglia-induced recruitment of reactive astrocytes leads to a detrimental effect on synapses, BBB and neurological outcome (Fig. 4-5). On the other hand, microglia-astrocyte crosstalk produces the release of the astrocytic protein TSP-1 that exerts beneficial effects on the recovery of synapses few days after injury (Fig. 6-7). Hence, pharmacological modulation of microglia-astrocyte interaction slow-down the progression of damage and, in turn, may accelerate long-term plasticity and rebuilding of neuronal network of the damaged area following TBI. Brake

Microglia are the resident immune cell in brain and have the necessary machinery to respond immediately to tissue damage under pathological conditions. Microglia morphology and function are closely related. After injury, microglial cells polarize to a M1 phenotype (pro-inflammatory) releasing cytokines such as TNF-α and IL-1β, or to a M2 phenotype (alternative/anti-inflammatory), in which microglial cells release IL-10 and/or TGF-β (44). Similarly, recent studies using gene transcriptome analysis have identified two different types of reactive astrocytes, named "A1" and "A2" (8,9,45). A1 astrocytes are observed after LPS-induced neuroinflammation and up-regulate many genes described to be destructive to synapses, suggesting a detrimental role. By contrast, A2 astrocytes are observed after ischemic stroke and increase the release of neurotrophic factors and thrombospondins that promote synapse repair, suggesting a neuroprotective role. Hence, the inflammatory response is not an isolated response of a single cell type but from a set of different cells that, as a whole, offer an orchestrated and fine-tune response after damage. Our data give evidence that the CHI model of TBI employed in this study induces a subtype of reactive microglia and astrocytes with "harmful" effects that might well correspond to the M1 and A1 reactive cells. The control of microglial inflammation exerts neuroprotective effects and has been extensively studied using several models in the last years (10,46,47). But our data support that both microglia and astrocytes are important in the pathophysiology of brain injuries since pharmacological TLR4 blockade and genetically non-active astrocytes from $IP_3R2^{-/-}$ have the opposite response. Using a traumatic brain injury model,

we demonstrate that microglia-to-astrocyte communication is necessary for: i) BBB stability and ii) synaptic reorganization in the surrounded area of lesion in pathological conditions. The pathological consequences of microglia-astrocyte interaction and its pharmacological blockade are discussed below.

Acute traumatic brain injury recruits excitable astrocytes surrounding the injury

The production of immunoreactive astrocytes during the pathogenesis of acute brain injuries (i.e. traumatic brain injury, ischemic stroke) has been extensively reported by anatomical and molecular techniques in several brain regions (8,13,48). In contrast, only few studies have explored the functional changes in the excitability of astrocytes following CNS injuries (13,49). By using *ex-vivo* Ca^{2+} imaging from TBI brain slices, we demonstrate that an increased number of excitable cortical astrocytes are recruited in the surrounding injured area within the first few hours following a brain damage. No changes in the frequency of the spontaneous responses was observed, suggesting that the astrocytic network is unaffected despite of the increase in extracellular glutamate after TBI, as previously reported (50). The increase in the amount of active astrocytes timely match the appearance of $GFAP^{+}$ astrocytes used as an anatomical indicator of astrocyte reactivity. Inhibition of microglia activation completely abolishes the recruitment of astrocytes with spontaneous Ca^{2+} responses with consequent improvement in synaptic number and BBB integrity. These data support the idea that reactive and active astrocytes induced by microglia activation result in aberrant loss of homeostatic functions shortly after an injury.

Microglia-astrocyte interaction regulates synaptic puncta following TBI

Over the past few years, several reports have implied a direct role of microglia and astrocyte in the control of synapses and modulation of neuronal network. For example, microglia activation of the complement cascade has been shown to control the mechanisms of synaptic pruning in neurons (35,51,52); while microglia-derived molecules (e.g. cytokines, neurotransmitters, and extracellular factors) were observed to regulate synaptic strength and neuronal activity after brain lesions or neurodegenerative diseases (16). In addition, it has been shown that microglia-released interleukin-1β induces synaptic facilitation through activation of neuronal NMDA receptors (14). Another study revealed that LPS application into brain slices leads to a rapid and transient

increase in the frequency of spontaneous synaptic AMPAergic current in CA1 neurons (15). Independent of the mechanism used by microglia to control synaptic transmission, these data indicate a crucial role of microglia in the control of neuronal networks. On the other hand, astrocytes also regulate synaptic transmission and neuronal homeostasis through several mechanisms (22,36,37,53). For example, astrocyte release of TSP-1/2 is associated with synapse formation and axonal outgrowth after stroke and partial sciatic ligation (13,31); while enhanced astrocytic production and release of D-serine or ephrins was observed to be detrimental to synapses after TBI (6,7). Here, we give strong evidence that the interaction between microglia and astrocyte regulates neuronal synapses following TBI through the activation of microglia via TLR4 receptors. TLR4 receptors are mainly implicated in the recognition of infectious pathogens or endogenous ligands released upon injury and are the main pathway to activate microglia after TBI. Although still debatable, recent molecular and genetic studies have confirmed that TLR4 are expressed exclusively by microglia in brain tissue and astrocytic response to activation of TLR4 seems to be totally dependent on the presence of microglia (9,15,54). In this way, microglial TLR4 activation by endogenous ligands released after TBI is crucial to establish a microglia-astrocyte crosstalk as evidenced by our data and from others. Supporting our hypothesis, we found that pharmacological blockage of microglial TLR4 signaling inhibits the recruitment of excitable astrocytes surrounding the injured area as well as decreases the amount of $GFAP^{+}$ astrocytes. We also observed that controlling the activation of microglia increases synaptic puncta in an astrocyte-dependent manner as $IP_3R2^{-/-}$ mice fail to recover synapses after blockage of TLR4 receptors. Third, microglia activation increases the release of the astrocyte-synaptogenic protein TSP-1 that plays a role in the homeostatic recovery of synapses in a sub-acute phase of the injury. Given all these evidence, our results indicate that activated microglia regulate synaptic transmission through an interaction with astrocytes after an acute brain injury.

Sub-acute effects of microglia-astrocyte interaction on synapses

Reactive astrocytes exert neuroprotective effects after TBI by limiting the extension of the injured core and by forming a glial scar (8). Our data extend the beneficial effects of reactive astrocytes to the recovery of synaptic number in a sub-acute phase of a traumatic brain injury. By using anatomical quantification of PSD-95/VGlut1 synaptic puncta, we demonstrate a homeostatic recovery of the initial synaptic loss a week following TBI (Fig. 5). This

physiological mechanism of synapse control seems to depend on the astrocyte activation as $IP_3R2^{-/-}$ mice continue to present reduced synaptic number. In addition, our data indicates that the mechanism controlling such synaptic regulation depends on the release of TSP-1 shortly after the injury. TSP-1 is a well-described astrocyte-released protein that serves to increase the number of neuronal synapses after a brain damage or during CNS diseases (42). In our experiments, we found that TSP-1 is transiently upregulated at 24 h after TBI, but its effect on synapse is observed only few days after injury. This data corroborate other studies suggesting that TSP-1 effect may take a several day period to be observed (42) as it acts on the expression of proteins that participate in the formation of new synaptic proteins rather than regulating cell adhesion proteins to lock synapses into place (i.e. stabilizing role) as previously suggested (31). So, while neuronal cortical synapses are rapidly lost after an injury (probably due to direct or indirect neuronal death), microglia-induced astrocyte activation increases the release of TSP1 in the first few hours to trigger the expression of neuronal synaptic proteins later on, leading to a partial recovery of synaptic loss 7 d.a.i. (Figure 5D). Interestingly, the synaptic recovery can be speed-up by an order of days after pharmacological blockage of the microglial TLR4 pathway (Fig 4E). Hence, TLR4 blockage of microglia-astrocyte interaction works to slow-down the progression of synaptic damage, thereby accelerating the recovery/repair of the surrounded damaged area.

Inhibition of microglia-astrocyte interaction improves BBB integrity after TBI

Both microglia and astrocytes physically interact with endothelial blood vessels in the brain influencing BBB integrity in diverse ways in health and disease (3). Here, we found that blocking the activation of the microglia-astrocyte interaction following TBI improves BBB integrity as determined by the decreased Evans Blue extravasation after microglial TLR4 inhibition in WT. In addition, we showed that TAK treatment does not decrease BBB breakdown in $IP_3R2^{-/-}$ mice, which indicates a direct effect of astrocyte on the neurovasculature, thereby corroborating previous findings that show a strong relationship between microglia-astrocyte interaction and BBB disruption (10,12). Moreover, the enhanced neuroprotective effect observed after TLR4 treatment in WT animals compared to $IP_3R2^{-/-}$ clearly indicates that microglia-astrocyte interaction also represents a key factor contributing to vascular integrity after TBI. The negative effect on the neurovasculature mediated by astrocytes could be explained by the release of vasoactive endothelial growth factor (VEGF) (55) or apolipoprotein E (APOE) (56) that have

been shown to exacerbate BBB damage. However, astrocytes are also known to release molecules that act beneficially on endothelia to reduce BBB permeability and promote its repair after CNS injury including Sonic hedgehog (Shh) (57) and retinoic acid (58). Such divergence of results demonstrate that astrocytes are pivotal regulators of endothelial BBB properties that act to open, maintain or restore barrier functions via specific molecular mechanisms that remain to be investigated.

Conclusion

Our data provide new evidences showing the crucial role of microglia-astrocyte interaction in the pathophysiology of brain injuries. We postulate that after a TBI, extracellular molecules that are rapidly released upon tissue damage activates microglial TLR4 signaling that serves as a signal to recruit excitable astrocytes in the peri-injured area. The microglia-induced reactive astrocytes will then affect neuronal excitability by modulating the number of synapses in a time-dependent manner. Shortly after the injury, astrocyte activity decreases the number of synapses probably to slow down the neuronal network and to avoid further neurotoxic damage. At the same time, active astrocytes release TSP-1 to promote synaptic recovery later on. After that, a homeostatic control of microglia activity may take place followed by a decrease in reactive and active astrocytes. Moreover, microglia-astrocyte interaction also exacerbates immediate BBB breakdown probably due to the release of astrocytic proteins and proinflammatory cytokines known to have detrimental effects on BBB. Overall, our data show that improvements on synaptic density and BBB integrity by decreasing microglia activation during the first few hours following a TBI could be used as a target for therapeutical treatments that may promote synaptic plasticity and improve cognitive function via astrocytic modulation.

Author contributions

JMR and JE conceived and designed the study. JMR and VFA performed and analysed experiments. JMR performed, analysed and wrote the scripts for Ca^{2+} imaging experiments. M.N. assisted with astrocyte imaging experiments and advised on calcium imaging analysis. APA, EFL and PNF assisted with $IP_3R2^{-/-}$ experiments. All authors revised the manuscript. JMR and JE wrote the manuscript.

Acknowledgments

This work was supported by grants from Fondo de Investigaciones Sanitarias (FIS) (ISCIII/FEDER) (Programa Miguel Servet II Grants CPII19/00005; PI16/00735; PI19/00082) and Fundación Mutua Madrileña to J.E. European Union's Horizon 2020 research and innovation programme under the Marie Sklodowska-Curie grant agreement No 794926 and Stop Fuga de Cerebros RochePharma to J.M.R. RTI2018-094887-B-I00 and RYC-2016-20414 to M.N. We thank Dr. Ju Chen (University of California, San Diego) and Dr. Gertrudis Perea (Cajal Institute Madrid, Spain), for kindly providing $IP_3R2^{-/-}$ animals and Dr. Juan Aguilar (HNP, Toledo, Spain) for technical support.

References

1. Carron SF, Alwis DS, Rajan R. Traumatic brain injury and neuronal functionality changes in sensory cortex. Front Syst Neurosci 2016;10:47.

2. Villapol S, Byrnes KR, Symes AJ. Temporal dynamics of cerebral blood flow, cortical damage, apoptosis, astrocyte-vasculature interaction and astrogliosis in the pericontusional region after traumatic brain injury. Front Neurol 2014;5:82.

3. Burda JE, Bernstein AM, Sofroniew MV. Astrocyte roles in traumatic brain injury. Exp Neurol 2016, Jan;275 Pt 3:305-15.

4. Clarke LE, Liddelow SA, Chakraborty C, Münch AE, Heiman M, Barres BA. Normal aging induces a1-like astrocyte reactivity. Proc Natl Acad Sci U S A 2018;115(8):E1896-905.

5. Ceyzériat K, Ben Haim L, Denizot A, Pommier D, Matos M, Guillemaud O, et al. Modulation of astrocyte reactivity improves functional deficits in mouse models of alzheimer's disease. Acta Neuropathol Commun 2018, Oct 16;6(1):104.

6. Nikolakopoulou AM, Koeppen J, Garcia M, Leish J, Obenaus A, Ethell IM. Astrocytic ephrin-b1 regulates synapse remodeling following traumatic brain injury. ASN Neuro 2016;8(1):1-18.

7. Perez EJ, Tapanes SA, Loris ZB, Balu DT, Sick TJ, Coyle JT, Liebl DJ. Enhanced astrocytic d-serine underlies synaptic damage after traumatic brain injury. J Clin Invest 2017, Aug 1;127(8):3114-25.

8. Shinozaki Y, Shibata K, Yoshida K, Shigetomi E, Gachet C, Ikenaka K, et al. Transformation of astrocytes to a neuroprotective phenotype by microglia via p2y1receptor downregulation. Cell Rep 2017;19(6):1151-64.

9. Liddelow SA, Guttenplan KA, Clarke LE, Bennett FC, Bohlen CJ, Schirmer L, et al. Neurotoxic reactive astrocytes are induced by activated microglia. Nature 2017;541(7638):481-7.
10. Donat CK, Scott G, Gentleman SM, Sastre M. Microglial activation in traumatic brain injury. Front Aging Neurosci 2017;9:208.
11. Ziebell JM, Adelson PD, Lifshitz J. Microglia: Dismantling and rebuilding circuits after acute neurological injury. Metab Brain Dis 2015, Apr;30(2):393-400.
12. Jha MK, Jo M, Kim J-H, Suk K. Microglia-Astrocyte crosstalk: An intimate molecular conversation. Neuroscientist 2018, Jun 1:1073858418783959.
13. Kim SK, Hayashi H, Ishikawa T, Shibata K, Shigetomi E, Shinozaki Y, et al. Cortical astrocytes rewire somatosensory cortical circuits for peripheral neuropathic pain. J Clin Invest 2016, May 2;126(5):1983-97.
14. Clark AK, Gruber-Schoffnegger D, Drdla-Schutting R, Gerhold KJ, Malcangio M, Sandkühler J. Selective activation of microglia facilitates synaptic strength. J Neurosci 2015, Mar 18;35(11):4552-70.
15. Pascual O, Ben Achour S, Rostaing P, Triller A, Bessis A. Microglia activation triggers astrocyte-mediated modulation of excitatory neurotransmission. Proc Natl Acad Sci U S A 2012, Jan 24;109(4):E197-205.
16. Béchade C, Cantaut-Belarif Y, Bessis A. Microglial control of neuronal activity. Front Cell Neurosci 2013;7:32.
17. Flierl MA, Stahel PF, Beauchamp KM, Morgan SJ, Smith WR, Shohami E. Mouse closed head injury model induced by a weight-drop device. Nat Protoc 2009;4(9):1328-37.
18. Ippolito DM, Eroglu C. Quantifying synapses: An immunocytochemistry-based assay to quantify synapse number. J Vis Exp 2010, Nov 16(45).
19. Perez-Alvarez A, Navarrete M, Covelo A, Martin ED, Araque A. Structural and functional plasticity of astrocyte processes and dendritic spine interactions. J Neurosci 2014, Sep 17;34(38):12738-44.
20. Nimmerjahn A, Kirchhoff F, Kerr JND, Helmchen F. Sulforhodamine 101 as a specific marker of astroglia in the neocortex in vivo. Nat Methods 2004, Oct;1(1):31-7.
21. Dorostkar MM, Dreosti E, Odermatt B, Lagnado L. Computational processing of optical measurements of neuronal and synaptic activity in networks. J Neurosci Methods 2010, Apr 30;188(1):141-50.

22. Rosa JM, Bos R, Sack GS, Fortuny C, Agarwal A, Bergles DE, et al. Neuron-glia signaling in developing retina mediated by neurotransmitter spillover. Elife 2015, Aug 14;4.
23. Navarrete M, Perea G, Fernandez de Sevilla D, Gómez-Gonzalo M, Núñez A, Martín ED, Araque A. Astrocytes mediate in vivo cholinergic-induced synaptic plasticity. PLoS Biol 2012, Feb;10(2):e1001259.
24. Albert-Weißenberger C, Várrallyay C, Raslan F, Kleinschnitz C, Sirén A-L. An experimental protocol for mimicking pathomechanisms of traumatic brain injury in mice. Exp Transl Stroke Med 2012, Feb 2;4:1.
25. Wu J, Zhao Z, Sabirzhanov B, Stoica BA, Kumar A, Luo T, et al. Spinal cord injury causes brain inflammation associated with cognitive and affective changes: Role of cell cycle pathways. J Neurosci 2014, Aug 13;34(33):10989-1006.
26. Zhang Y, Chen K, Sloan SA, Bennett ML, Scholze AR, O'Keeffe S, et al. An rna-sequencing transcriptome and splicing database of glia, neurons, and vascular cells of the cerebral cortex. J Neurosci 2014, Sep 3;34(36):11929-47.
27. Zhang Y, Sloan SA, Clarke LE, Caneda C, Plaza CA, Blumenthal PD, et al. Purification and characterization of progenitor and mature human astrocytes reveals transcriptional and functional differences with mouse. Neuron 2016, Jan 6;89(1):37-53.
28. Bennett ML, Bennett FC, Liddelow SA, Ajami B, Zamanian JL, Fernhoff NB, et al. New tools for studying microglia in the mouse and human CNS. Proc Natl Acad Sci U S A 2016, Mar 22;113(12):E1738-46.
29. Ohsumi A, Nawashiro H, Otani N, Ooigawa H, Toyooka T, Shima K. Temporal and spatial profile of phosphorylated connexin43 after traumatic brain injury in rats. J Neurotrauma 2010, Jul;27(7):1255-63.
30. Perez EJ, Cepero ML, Perez SU, Coyle JT, Sick TJ, Liebl DJ. EphB3 signaling propagates synaptic dysfunction in the traumatic injured brain. Neurobiol Dis 2016, Oct;94:73-84.
31. Liauw J, Hoang S, Choi M, Eroglu C, Choi M, Sun G-H, et al. Thrombospondins 1 and 2 are necessary for synaptic plasticity and functional recovery after stroke. J Cereb Blood Flow Metab 2008, Oct;28(10):1722-32.
32. Min H, Hong J, Cho I-H, Jang YH, Lee H, Kim D, et al. TLR2-induced astrocyte MMP9 activation compromises the blood brain barrier and exacerbates intracerebral hemorrhage in animal models. Mol Brain 2015, Apr 10;8:23.

33. Petravicz J, Boyt KM, McCarthy KD. Astrocyte ip3r2-dependent ca(2+) signaling is not a major modulator of neuronal pathways governing behavior. Front Behav Neurosci 2014;8:384.
34. Srinivasan R, Huang BS, Venugopal S, Johnston AD, Chai H, Zeng H, et al. Ca(2+) signaling in astrocytes from ip3r2(-/-) mice in brain slices and during startle responses in vivo. Nat Neurosci 2015, May;18(5):708-17.
35. Wake H, Moorhouse AJ, Jinno S, Kohsaka S, Nabekura J. Resting microglia directly monitor the functional state of synapses in vivo and determine the fate of ischemic terminals. J Neurosci 2009, Apr 1;29(13):3974-80.
36. Perea G, Navarrete M, Araque A. Tripartite synapses: Astrocytes process and control synaptic information. Trends Neurosci 2009, Aug;32(8):421-31.
37. Araque A, Carmignoto G, Haydon PG, Oliet SHR, Robitaille R, Volterra A. Gliotransmitters travel in time and space. Neuron 2014, Feb 19;81(4):728-39.
38. Susarla BTS, Villapol S, Yi J-H, Geller HM, Symes AJ. Temporal patterns of cortical proliferation of glial cell populations after traumatic brain injury in mice. ASN Neuro 2014, May 8;6(3):159-70.
39. Ding M-C, Wang Q, Lo EH, Stanley GB. Cortical excitation and inhibition following focal traumatic brain injury. J Neurosci 2011, Oct 5;31(40):14085-94.
40. Johnstone VPA, Wright DK, Wong K, O'Brien TJ, Rajan R, Shultz SR. Experimental traumatic brain injury results in long-term recovery of functional responsiveness in sensory cortex but persisting structural changes and sensorimotor, cognitive, and emotional deficits. J Neurotrauma 2015, Sep 1;32(17):1333-46.
41. Johnstone VPA, Yan EB, Alwis DS, Rajan R. Cortical hypoexcitation defines neuronal responses in the immediate aftermath of traumatic brain injury. PLoS One 2013;8(5):e63454.
42. Christopherson KS, Ullian EM, Stokes CCA, Mullowney CE, Hell JW, Agah A, et al. Thrombospondins are astrocyte-secreted proteins that promote CNS synaptogenesis. Cell 2005, Feb 11;120(3):421-33.
43. Cheng C, Yu Z, Zhao S, Liao Z, Xing C, Jiang Y, et al. Thrombospondin-1 gene deficiency worsens the neurological outcomes of traumatic brain injury in mice. Int J Med Sci 2017;14(10):927-36.
44. Davis EJ, Foster TD, Thomas WE. Cellular forms and functions of brain microglia. Brain Res Bull 1994;34(1):73-8.

45. Zamanian JL, Xu L, Foo LC, Nouri N, Zhou L, Giffard RG, Barres BA. Genomic analysis of reactive astrogliosis. J Neurosci 2012, May 2;32(18):6391-410.
46. Alawieh A, Langley EF, Weber S, Adkins D, Tomlinson S. Identifying the role of complement in triggering neuroinflammation after traumatic brain injury. J Neurosci 2018;38(10):2519-32.
47. Parada E, Casas AI, Palomino-Antolin A, Gómez-Rangel V, Rubio-Navarro A, Farré-Alins V, et al. Early toll-like receptor 4 blockade reduces ROS and inflammation triggered by microglial pro-inflammatory phenotype in rodent and human brain ischaemia models. Br J Pharmacol 2019, Aug;176(15):2764-79.
48. Carron SF, Yan EB, Alwis DS, Rajan R. Differential susceptibility of cortical and subcortical inhibitory neurons and astrocytes in the long term following diffuse traumatic brain injury. J Comp Neurol 2016, Dec 1;524(17):3530-60.
49. Takatsuru Y, Eto K, Kaneko R, Masuda H, Shimokawa N, Koibuchi N, Nabekura J. Critical role of the astrocyte for functional remodeling in contralateral hemisphere of somatosensory cortex after stroke. J Neurosci 2013, Mar 13;33(11):4683-92.
50. Cantu D, Walker K, Andresen L, Taylor-Weiner A, Hampton D, Tesco G, Dulla CG. Traumatic brain injury increases cortical glutamate network activity by compromising gabaergic control. Cereb Cortex 2015, Aug;25(8):2306-20.
51. Tremblay M-È, Lowery RL, Majewska AK. Microglial interactions with synapses are modulated by visual experience. PLoS Biol 2010, Nov 2;8(11):e1000527.
52. Schafer DP, Lehrman EK, Stevens B. The "quad-partite" synapse: Microglia-synapse interactions in the developing and mature CNS. Glia 2013, Jan;61(1):24-36.
53. Navarrete M, Cuartero MI, Palenzuela R, Draffin JE, Konomi A, Serra I, et al. Astrocytic p38α MAPK drives NMDA receptor-dependent long-term depression and modulates long-term memory. Nat Commun 2019, Jul 4;10(1):2968.
54. Holm TH, Draeby D, Owens T. Microglia are required for astroglial toll-like receptor 4 response and for optimal TLR2 and TLR3 response. Glia 2012, Apr;60(4):630-8.
55. Argaw AT, Gurfein BT, Zhang Y, Zameer A, John GR. VEGF-mediated disruption of endothelial CLN-5 promotes blood-brain barrier breakdown. Proc Natl Acad Sci U S A 2009, Feb 10;106(6):1977-82.

56. Bell RD, Winkler EA, Singh I, Sagare AP, Deane R, Wu Z, et al. Apolipoprotein E controls cerebrovascular integrity via cyclophilin A. Nature 2012, May 16;485(7399):512-6.
57. Alvarez JI, Dodelet-Devillers A, Kebir H, Ifergan I, Fabre PJ, Terouz S, et al. The hedgehog pathway promotes blood-brain barrier integrity and CNS immune quiescence. Science 2011, Dec 23;334(6063):1727-31.
58. Mizee M, Nijland P, van der Pol SM, van Het Hof B, Mebius R, van Horseen J, et al. Astrocyte-derived retinoic acid: A novel regulator of blood-brain barrier function in multiple sclerosis. <u>Acta Neuropathol</u> 2014;128(5):691-703.
59. Paxinos G, Franklin K. Paxinos and franklin's the mouse brain in stereotaxic coordinates. 5th Edition ed. San Diego: Elsevier Academic Press; 2019.

Figure legends

Figure 1: Moderate traumatic brain injury causes significant increase in astrogliosis and microglia activation. (A) Top: Schematic diagram showing the experimental strategy for the injury and brain slice (adapted from (59)). Dotted black box represents injured area within motor and somatosensory (S1) cortex. Red dotted box represents where functional and anatomical experiments are performed. Images in a' and a'' are from area delimited in the dotted black rectangle. Bottom: Nissl staining tissues showing gross morphological damage 24 h after sham (a') or TBI (a'') injury. Scale bar: 20 µm. (B) High magnification confocal images of S1 cortex immunostained with a marker for astrocytes (GFAP, green) or microglia (Iba-1, red) in contra and ipsilateral S1 cortex. On the right, insets from individual microglia cells displaying resting (ramified morphology) or activated (hypertrophic or bushy morphology) phenotypes. Scale bar: 5 µm. Yellow arrow represents a bushy microglia phenotype represented on the right. Sections were counterstained with DAPI (blue) to illustrate nuclei. (C) Corresponding $GFAP^+$ quantification in sham (n = 6) and TBI (n = 5) mice. Increased astrocyte reactivity (GFAP), a hallmark of brain injury, is observed in ipsilateral S1 after TBI as compared with sham mice and contralateral TBI-cortex. (D) Unbiased stereological quantitative assessment of microglial phenotypes in the S1 cortex from sham (n = 6 TBI) and TBI (n = 5 TBI). Values are mean ± SEM. One-way ANOVA, Tukey post-hoc test * $p < 0.05$, ** $p < 0.01$, *** $p < 0.001$.

Figure 2: Pharmacological blockage of microglial TLR4 receptors decreases astrocyte reactivity in S1 cortex. (A) Schematic diagram showing the experimental strategy for the injury and brain slice as well as the timing of the pharmacological treatment. TAK242 or vehicle were i.p. injected one hour after injury to block TLR4 receptors activation. (B) Confocal images of S1 cortex immunostained with a marker for astrocytes (GFAP, green) and microglia (Iba-1, red) in the contralateral (contra) and ipsilateral (ipsi) S1 cortex from TBI mice treated with vehicle (left) or TAK242 (right) 1 hour after injury. Sections were counterstained with DAPI (blue) to illustrate nuclei. Scale bar: 20 µm. (C) Corresponding measurements of reactive astrocytes in contra and ipsilateral S1 cortex following TBI in mice treated with vehicle or TAK242. (D) Unbiased stereological quantitative assessment of microglial phenotypes in the S1 cortex from

vehicle or TAK242 treated mice. n = 5 TBI/Vehicle and n = 5 TBI/TAK. Values are mean ± SEM. One-way ANOVA, Tukey post-hoc test, *$p < 0.05$, ** $p < 0.01$ and ***$p < 0.001$.

Figure 3: Traumatic brain injury recruits active astrocytes through activation of microglia. (A) Schematic of the Ca^{2+} imaging experiments showing the cortical area where astrocyte activity is registered. (B) Left: fluorescent intensities of a TBI S1 cortex loaded with Fluo4-AM (1µg/µL) and heat maps of maximal ΔF/F before and during a spontaneous activity indicated in the rightmost figure. Color scale indicates normalized changes in fluorescence during spontaneous activity. Scale bar: 10 µm. Right: time course of the spontaneous Ca^{2+} oscillations from astrocytes indicated on the left. (C) Proportion of active astrocytes that showed at least one Ca^{2+} event during a 1-min recording period in sham (n = 5 animals/432 ROIs) and TBI-mice (contra- and ipsilateral cortex, n = 5 animals/576 ROIs and n = 6 animals/480 ROIs, respectively). (D) Top: Raster-plot showing the relative change in fluorescence (ΔF/F) in astrocytes for 48 ROIs taken from a random field of view (FOV). Bottom: Histogram denotes individual events over time form ROIs with responsive Ca^{2+} transients. Color scale indicates normalized changes in fluorescence during spontaneous activity. (E) Corresponding Ca^{2+} transient frequency in sham and TBI-mice. (F) Schematic of fluorescent experiments: TBI was performed 1 h before the administration of vehicle or TAK242 (i.p.) and 24 h later, brain was removed and sliced to proceed the astrocyte loading with the calcium dye Fluo4-AM as in A. (G) Proportion of active astrocytes that showed at least one Ca^{2+} event during a 1-min recording period in vehicle (n = 4 animals, contra: 432 ROIs and ipsi: 480 ROIs) or TAK242 (n = 5 animals, contra: 336 ROIs and ipsi: 720 ROIs) group. (H) Corresponding frequency of Ca^{2+} transients. Values are mean ± SEM. One-way ANOVA, Tukey post-hoc test, ** $p < 0.01$, ***$p < 0.001$.

Figure 4: Control of microglia-astrocyte interaction improves synaptic loss and prevents blood-brain barrier damage after TBI. (A) Top: Schematic diagram showing the experimental strategy. Bottom: Bar graph showing the effect of vehicle or TAK242 administration on the levels of S100β in plasma. (B) Illustration of three distinct coronal sections through the TBI center showing the Evans Blue distribution throughout a vehicle or TAK-treated mouse brain. (C) Blood-brain barrier integrity assessed by Evans Blue extravasations (mm^3) 24 h after TBI in the contralateral (contra) and ipsilateral (ipsi) brain of WT (left) or $IP_3R2^{-/-}$ (right) mice treated with

vehicle (WT = 8, $IP_3R2^{-/-}$ = 4) or TAK242 (WT = 6, $IP_3R2^{-/-}$ = 4)). (D) Representative confocal images of synapses (white arrowheads) indicated by colocalization of presynaptic (VGlut1, green) and postsynaptic (PSD-95, red) markers in sham and TBI ipsilateral S1 cortex. Scale bar: 5 µm. (E) Quantitative analysis showing decreased in the number of synaptic puncta 24 h after TBI in WT (white bars) and $IP_3R2^{-/-}$ (grey bars) mice (n = 12 FOV/4 mice group in WT and n = 10 FOV/3 mice group). Values are mean ± SEM. One-way ANOVA, Tukey post-hoc test, * $p < 0.05$, ** $p < 0.01$, *** $p < 0.001$.

Figure 5: Homeostatic sub-acute recovery of astrocyte activity and synaptic density in TBI brain 7 days after TBI. (A) Schematic diagram showing the experimental strategy. (B) Left: Percentage of active astrocytes (left) and number of Ca^{2+} oscillations (right) in contra and ipsilateral cortex of sham (n = 3) or TBI mice (n = 4) 7 days after the injury. (C) Percentage of $GFAP^{+}$ astrocytes in contra and ipsilateral cortex of TBI mice 7 days after injury. (D) Unbiased stereological quantitative assessment of microglial phenotypes (Iba-1 staining) in the S1 cortex from sham and TBI mice. (n = 6 sham and n = 5 TBI for GFAP and Iba-1 staining). (E) Quantitative analysis showing homeostatic recovery of synaptic puncta density 7 days after TBI (n = 9 FOV from 3 mice). Values are mean ± SEM. One-way ANOVA, Tukey post-hoc test * $p < 0.05$, ** $p < 0.01$, *** $p < 0.001$.

Figure 6: Transient up-regulation of TSP-1 in S1 cortex following TBI. (A) Top, Western blots of TSP-1 and actin from sham, two vehicle (Veh) and two treated mice (TAK). Bottom, semi-quantitative analysis of TSP-1 immunoreactivity showing an upregulation of TSP-1 24 h after the TBI and its reduction after blocking microglia activation (TAK; n = 4 sham group, n = 5 vehicle group, n = 6 TAK group). (B) Quantification of PSD-95/VGlut1 synaptic puncta from $IP_3R2^{-/-}$ mice (sham = 3 and TBI = 3). (C) Effects of microglia-induced astrocyte reactivity on neurological severity scores (NSS) in WT and $IP_3R2^{-/-}$ mice. Mice were subjected to TBI followed by treatment of vehicle (n = 12 WT group, n = 3 in $IP_3R2^{-/-}$ group) or TAK242 (n = 9 WT group, n = 3 in $IP_3R2^{-/-}$ group). NSS evaluated at 1 and 24 h after the injury. Values are mean ± SEM. * $p < 0.05$, ** $p < 0.01$ and ** $p< 0.001$, 1-way ANOVA.

Figure 7: Schematic diagram of the microglia-astrocyte interaction following TBI. Microglia-astrocyte interaction represents a key physiological mechanism to regulate both neuronal vasculature and synaptic number following TBI in a time-dependent manner. Shortly after the injury, astrocyte activity decreases the number of synapses probably to slow down the neuronal network and avoid further neurotoxic damage. At the same time, active astrocytes release TSP-1 to promote synaptic recovery later on. After this, a homeostatic control of microglia activity may take place followed by a decrease in active astrocytes and neuronal excitability. Moreover, microglia-astrocyte interaction also exacerbates immediate BBB breakdown probably due to the release of astrocytic proteins and proinflammatory cytokines known to have detrimental effects on BBB.

FIGURE 1

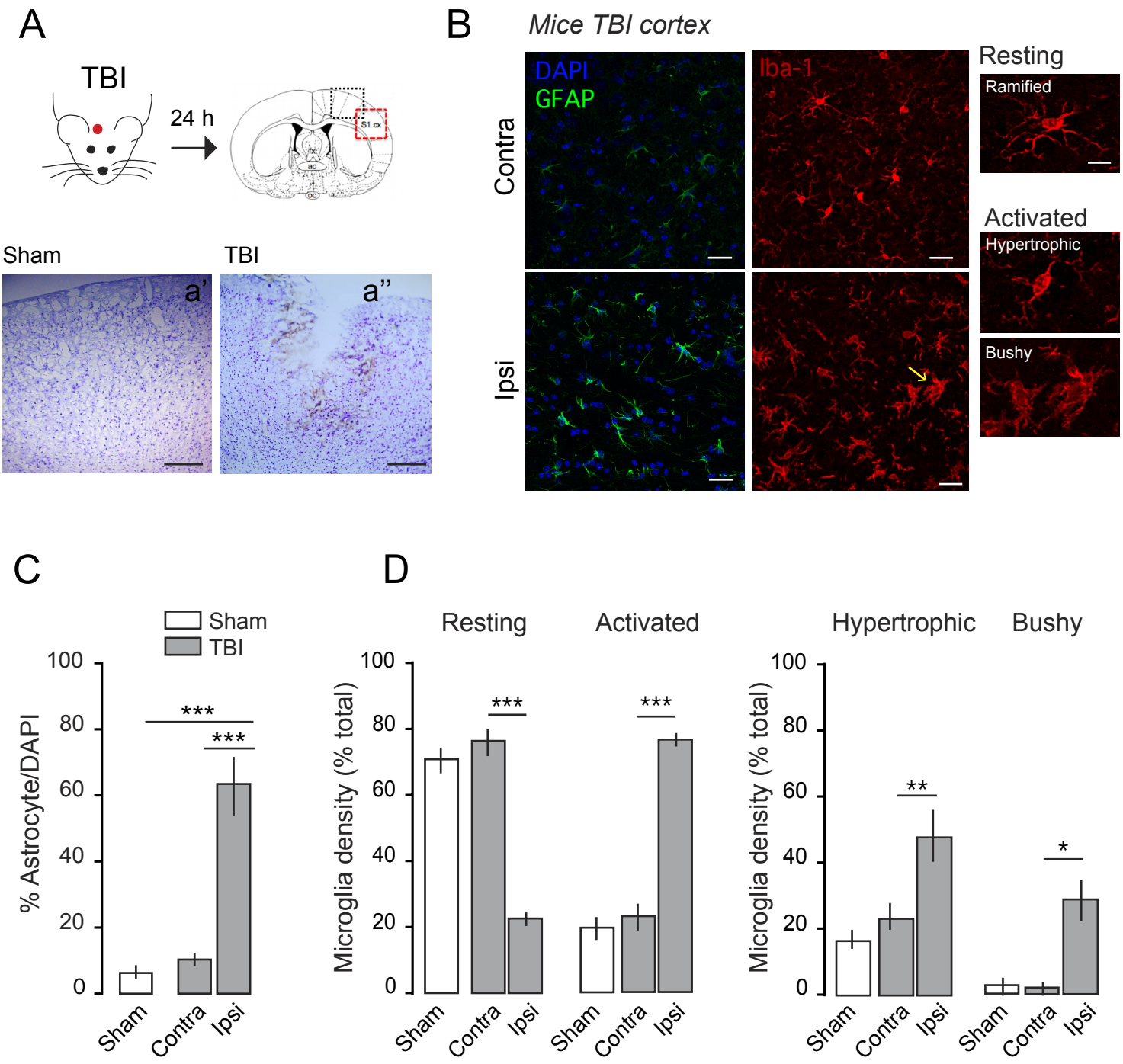
A
TBI
24 h
S1 cx
Sham
TBI
a'
a''
B
Mice TBI cortex
DAPI
GFAP
Iba-1
Contra
Ipsi
Resting
Ramified
Activated
Hypertrophic
Bushy
C
Sham
TBI
% Astrocyte/DAPI
100
80
60
40
20
0
***
***
Sham
Contra
Ipsi
D
Resting
Activated
Hypertrophic
Bushy
Microglia density (% total)
***
***
**
*
Sham
Contra
Ipsi

FIGURE 2

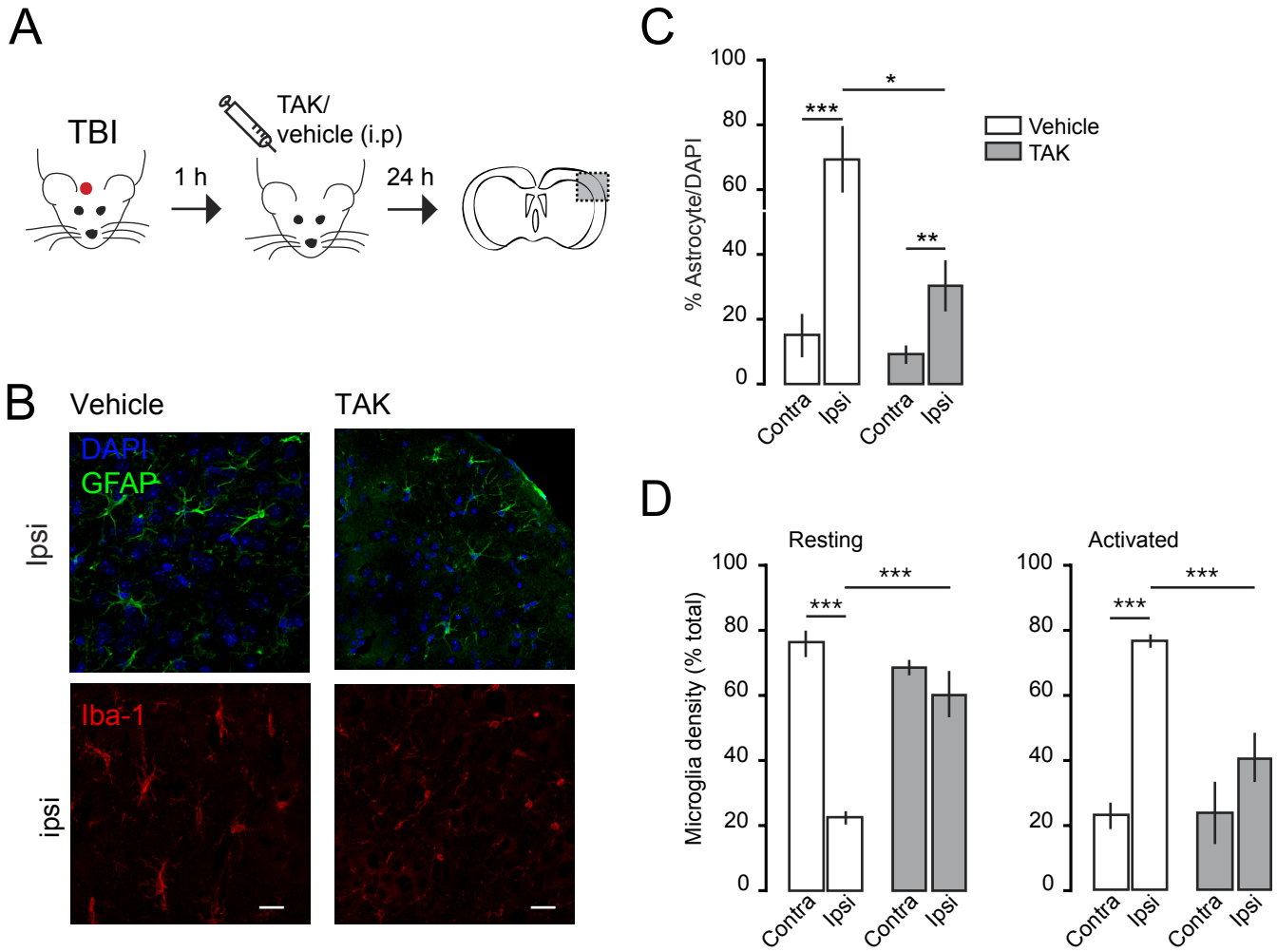
A
TBI
1 h
TAK/
vehicle (i.p)
24 h
B
Vehicle
TAK
DAPI
GFAP
Ipsi
Iba-1
ipsi
C
% Astrocyte/DAPI
100
80
60
40
20
0
***
*
**
Vehicle
TAK
Contra
Ipsi
Contra
Ipsi
D
Resting
Activated
Microglia density (% total)
100
80
60
40
20
0
***
***
***
***
Contra
Ipsi
Contra
Ipsi
Contra
Ipsi
Contra
Ipsi

FIGURE 3

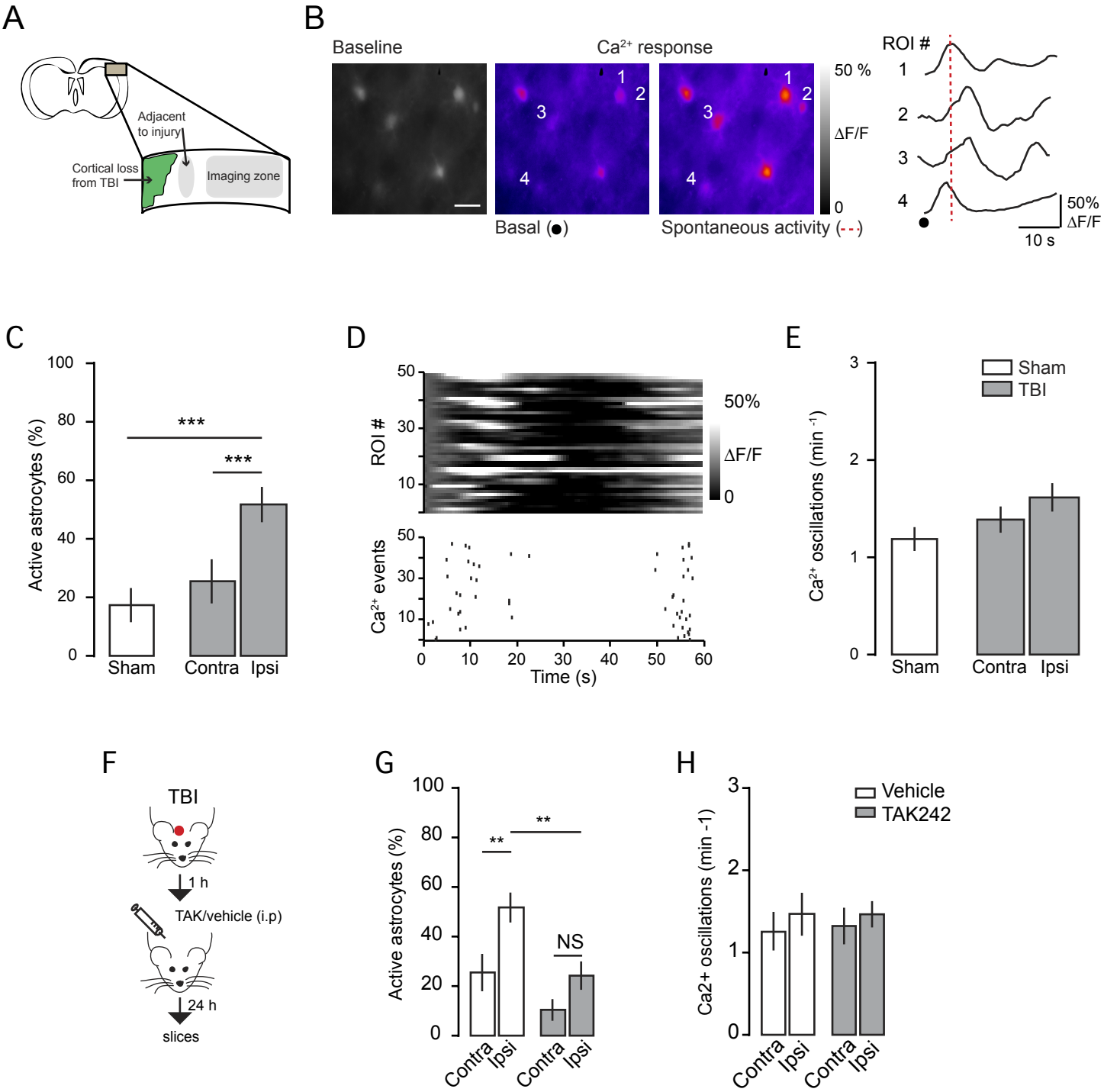
A
Adjacent to injury
Cortical loss from TBI
Imaging zone
B
Baseline
Ca2+ response
50 %
ΔF/F
0
ROI #
1
2
3
4
Basal (●)
Spontaneous activity (- - -)
50% ΔF/F
10 s
C
Active astrocytes (%)
100
80
60
40
20
0
***
***
Sham
Contra
Ipsi
D
ROI #
50
30
10
50%
ΔF/F
0
Ca2+ events
Time (s)
0
10
20
30
40
50
60
E
Ca2+ oscillations (min -1)
3
2
1
0
Sham
TBI
Sham
Contra
Ipsi
F
TBI
1 h
TAK/vehicle (i.p)
24 h
slices
G
Active astrocytes (%)
100
80
60
40
20
0
**
**
NS
Contra
Ipsi
Contra
Ipsi
H
Ca2+ oscillations (min -1)
3
2
1
0
Vehicle
TAK242
Contra
Ipsi
Contra
Ipsi

FIGURE 4

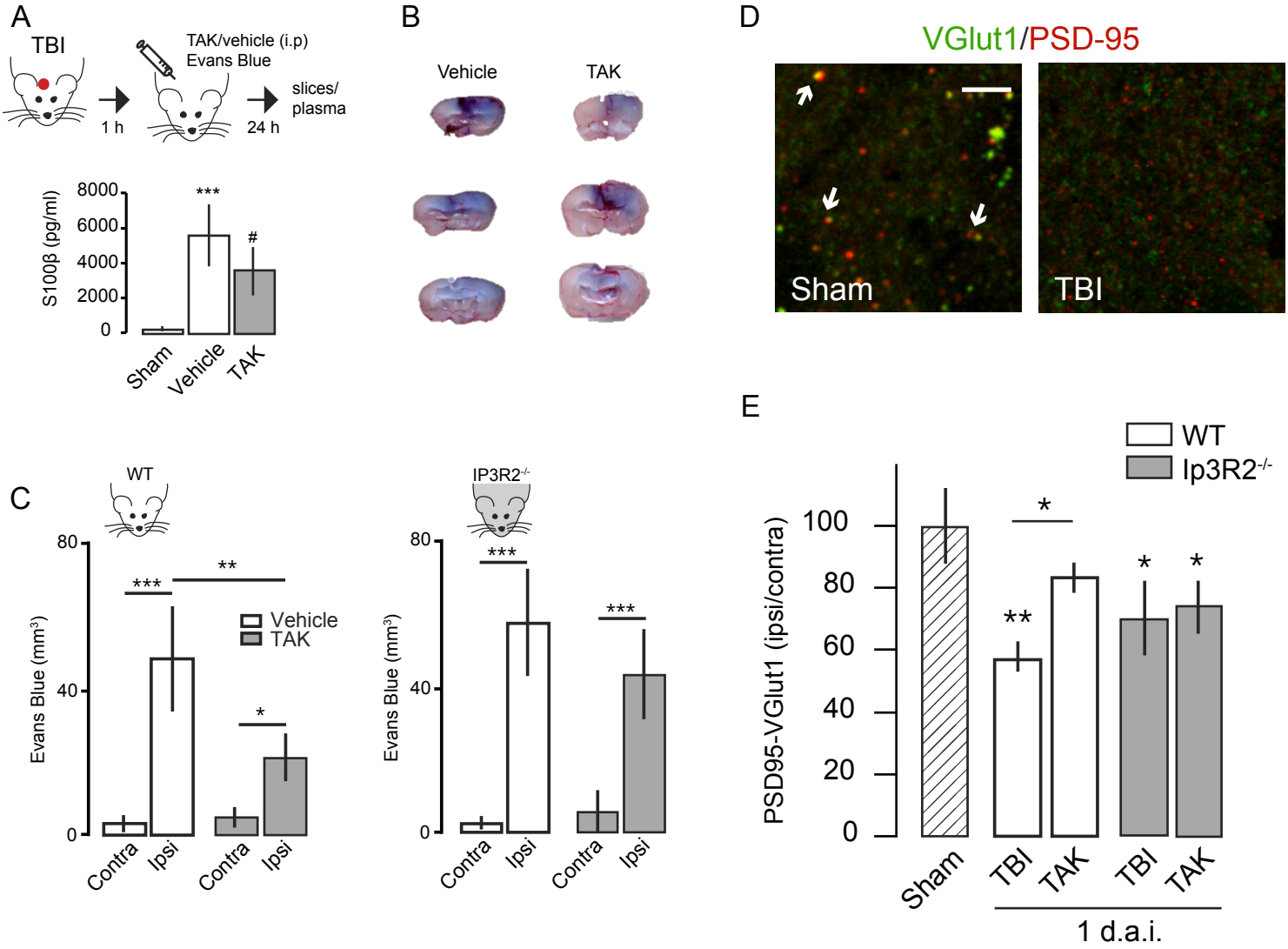
A
TBI
1 h
TAK/vehicle (i.p)
Evans Blue
24 h
slices/
plasma
S100β (pg/ml)
8000
6000
4000
2000
0
***
#
Sham
Vehicle
TAK
B
Vehicle
TAK
D
VGlut1/PSD-95
Sham
TBI
C
WT
IP3R2-/-
Evans Blue (mm3)
80
40
0
***
**
*
Vehicle
TAK
Contra
Ipsi
E
WT
Ip3R2-/-
PSD95-VGlut1 (ipsi/contra)
100
80
60
40
20
0
*
**
Sham
TBI
TAK
1 d.a.i.

FIGURE 5

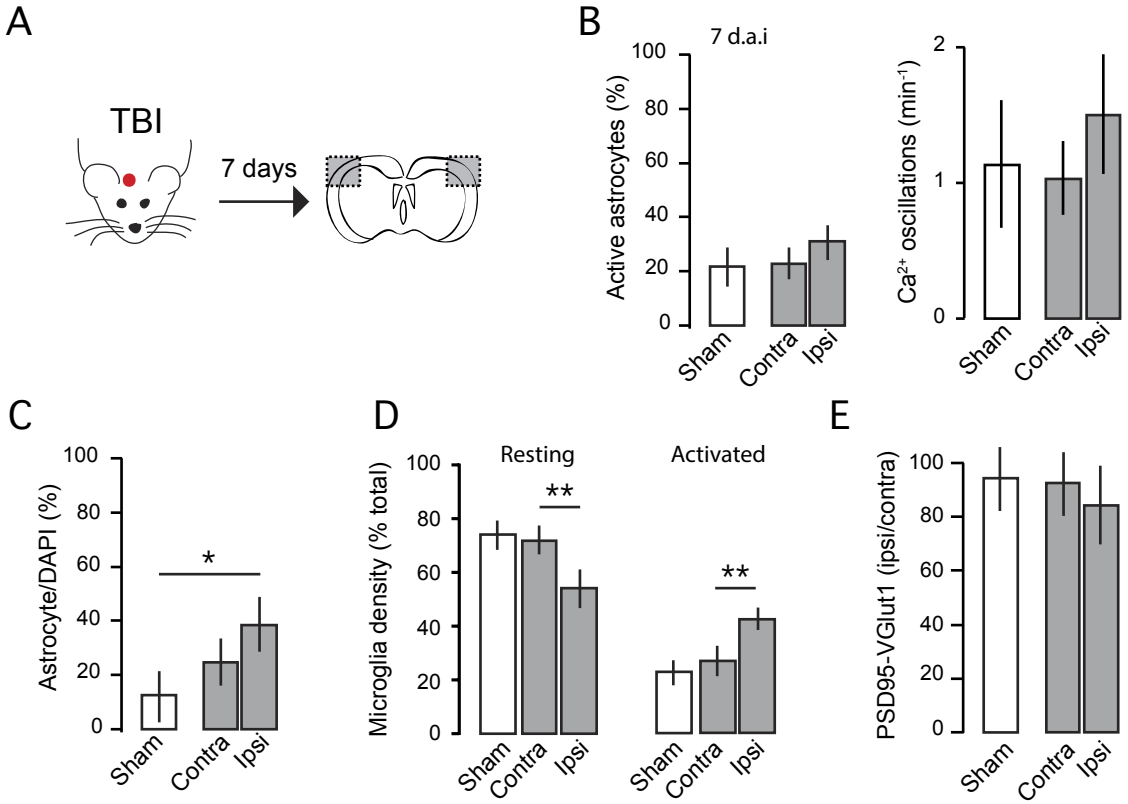
A
TBI
7 days
B
7 d.a.i
Active astrocytes (%)
100
80
60
40
20
0
Sham
Contra
Ipsi
Ca2+ oscillations (min-1)
2
1
0
Sham
Contra
Ipsi
C
Astrocyte/DAPI (%)
100
80
60
40
20
0
*
Sham
Contra
Ipsi
D
Resting
Activated
Microglia density (% total)
100
80
60
40
20
0
**
**
Sham
Contra
Ipsi
Sham
Contra
Ipsi
E
PSD95-VGlut1 (ipsi/contra)
100
80
60
40
20
0
Sham
Contra
Ipsi

FIGURE 6

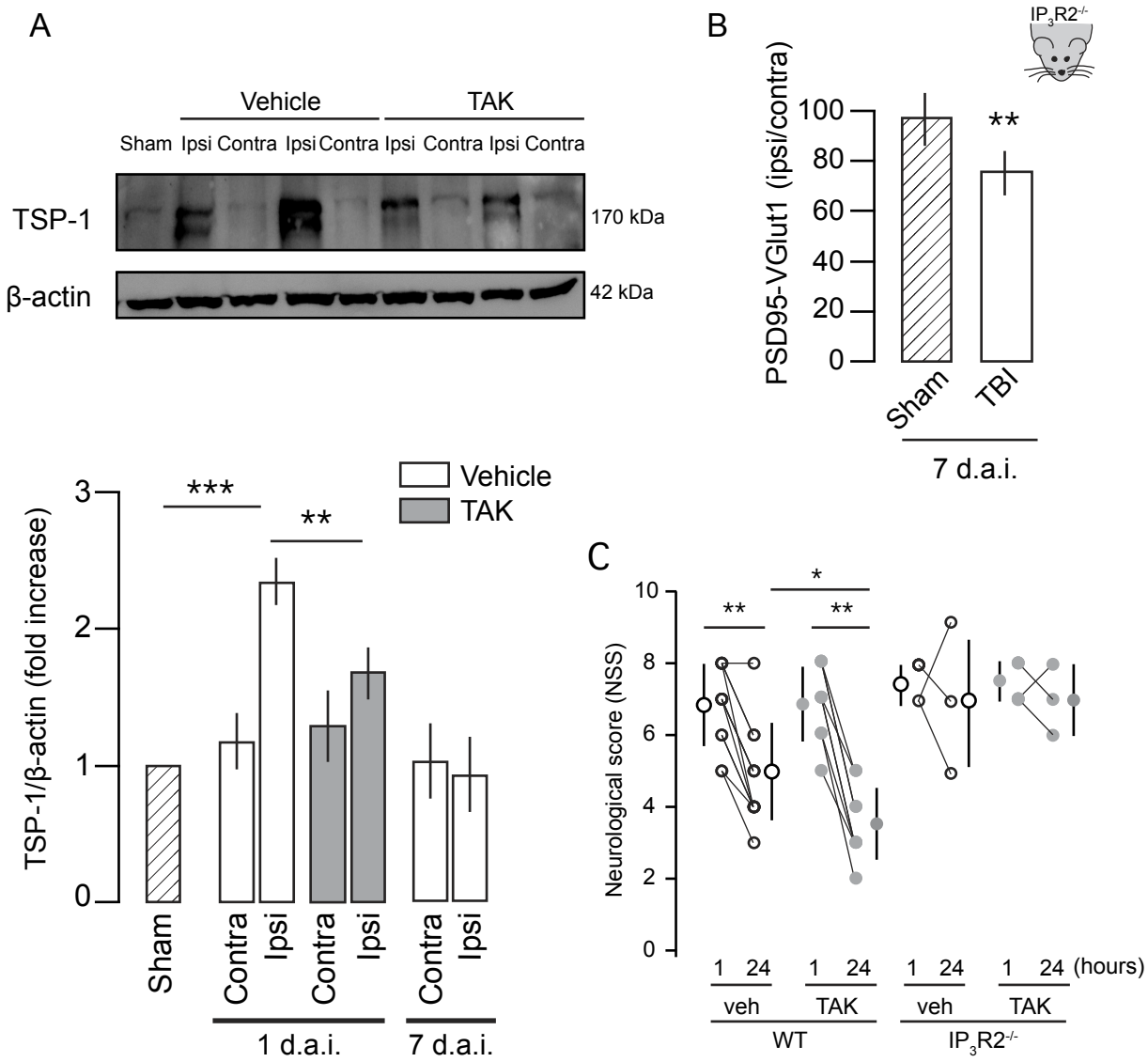
A
Vehicle
TAK
Sham Ipsi Contra Ipsi Contra Ipsi Contra Ipsi Contra
TSP-1
170 kDa
β-actin
42 kDa
B
IP3R2-/-
PSD95-VGlut1 (ipsi/contra)
100
80
60
40
20
0
**
Sham
TBI
7 d.a.i.
Vehicle
TAK
TSP-1/β-actin (fold increase)
3
2
1
0
***
**
Sham
Contra
Ipsi
Contra
Ipsi
Contra
Ipsi
1 d.a.i.
7 d.a.i.
C
Neurological score (NSS)
10
8
6
4
2
0
**
*
**
1 24 1 24 1 24 1 24 (hours)
veh TAK veh TAK
WT
IP3R2-/-

FIGURE 7

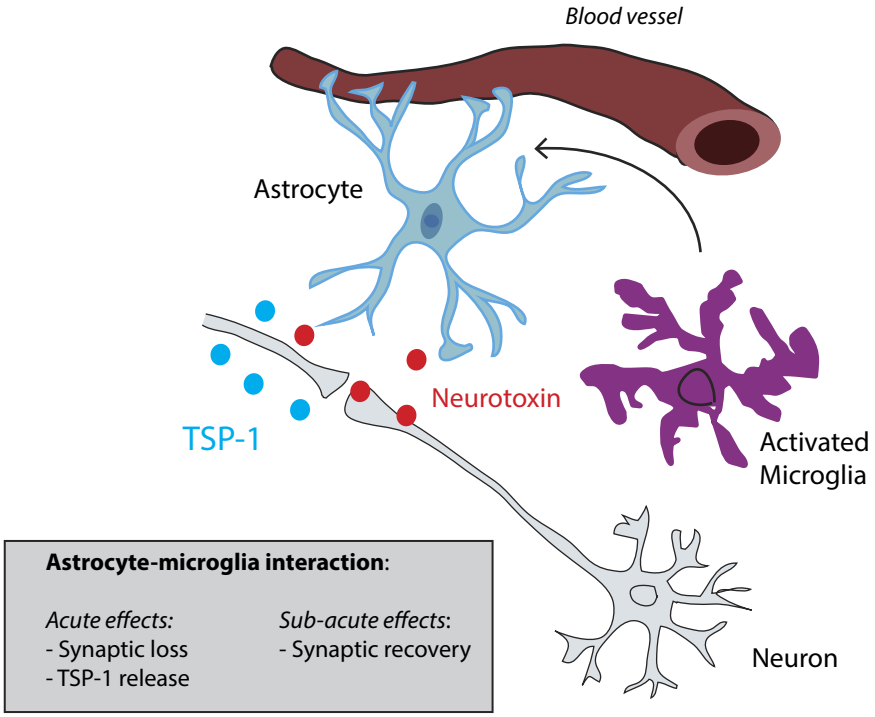
Blood vessel
Astrocyte
Neurotoxin
TSP-1
Activated
Microglia
Neuron
Astrocyte-microglia interaction:
Acute effects:
- Synaptic loss
- TSP-1 release
Sub-acute effects:
- Synaptic recovery